Device-Free Simultaneous Wireless Localization and Activity Recognition With Wavelet Feature

Jie Wang, *Member, IEEE*, Xiao Zhang, Qinghua Gao, Xiaorui Ma, Xueyan Feng, and Hongyu Wang

***Abstract*—Device-Free simultaneous wireless Localization and Activity Recognition (DFLAR) is a promising novel technique that empowers wireless networks with the ability to perceive the location and activity of a target within its deployment area while not equipping the target with a device. This technique turns traditional wireless networks into smart context-aware networks and will play an important role in many smart applications, e.g., smart city, smart space, and smart house. Essentially, DFLAR utilizes the shadowing effect incurred by the target on wireless links to realize localization and activity recognition. The feature utilized to characterize the shadowing effect is crucial for DFLAR. Traditional methods use time-domain features to characterize the shadowing effect. In this paper, we explore the method of realizing DFLAR with a wavelet feature. Compared with the time-domain feature, the wavelet feature could characterize link measurement in both the time and frequency domains, which could provide in-depth robust discriminative information and, therefore, improve the performance of the DFLAR system. Meanwhile, we also design a two-stage strategy to realize multitarget DFLAR with the feature map built by one target only, which reduces the training complexity remarkably. The experimental results in a clutter indoor scenario show that it could achieve location estimation and activity recognition accuracy of higher than 90%.**

***Index Terms*—Activity recognition, device-free localization (DFL), wavelet feature, wireless localization.**

I. Introduction

With the popularization of wireless networks, no matter where we are, there are wireless links around us that connect us with each other. All these links form a large network that perceives the event that occurs within its deployment area silently. When a target moves within the deployment area of the network, it will shadow some wireless links unavoidably and cause variation of the wireless signals. When a target locates at different locations or performs different activities, the showed signals will be different. Thus, it is feasible to realize device-free localization (DFL) or device-free activity recognition (DFAR) based on wireless link measurement information. DFL and DFAR techniques have overstepped the traditional communication task of wireless networks and made them smart context-aware networks with the ability to perceive the location and activity of a target within its deployment area while not equipping the target with a device. With the development of these techniques, they will play an important role in many smart applications, e.g., smart city, smart space, and smart house.

Most of the DFL techniques use time-domain received signal strength (RSS) variation, e.g., mean, variance, or peak-to-peak value of RSS, caused by the shadowing effect of the target on wireless links to realize location estimation. More recently, these time-domain features have been also explored and utilized to realize DFAR. The aforementioned work makes valuable exploration and enables wireless networks with the ability of being context aware. However, as a novel emerging technique, there are still several problems to solve. One fundamental problem is how to build a robust and discriminative feature to characterize the shadowing effect. Although the time-domain feature could well describe the shadowing effect, it is sensitive to environmental noise. In clutter indoor scenarios, the performance of DFL or DFAR will remarkably drop. To solve this problem, we explore the method of realizing Device-Free simultaneous wireless Localization and Activity Recognition (DFLAR) with the wavelet feature. Specifically, we use the number of zero crossing points (ZCPs), variance, and energy of the approximation coefficient vector cA_4 and detailed coefficient vector cD_4 of the fourth wavelet decomposition level to build the feature vector. Compared with traditional features, the proposed feature could provide in-depth robust discriminative information and, therefore, improve the performance of the DFLAR system. Another important problem is how to realize DFLAR efficiently. To realize activity recognition, one has to use machine learning methods. However, the training complexity exponentially increases with the number of targets. This makes the multitarget DFLAR a complex and challenging problem. In this paper, we first achieve coarse target detection and DFL with simple geometry method whose complexity is invariable with the number of targets. Then, we realize accurate localization and activity recognition simultaneously with the softmax regression method for each target one by one by taking the coarse estimation as constraint information. The constraint information not only identifies different targets but makes it possible to realize multitarget DFLAR with a traditional single-target feature map as well, which only needs to collect the features with one target performing the training task. This makes the complexity of the system linear with the number of targets.

With the aforementioned schemes, the proposed DFLAR framework could achieve robust and better performance. We

Manuscript received September 21, 2015; revised January 13, 2016; accepted April 16, 2016. Date of publication April 21, 2016; date of current version February 10, 2017. This work was supported in part by the National Natural Science Foundation of China under Grant 61301130 and Grant 61401059, by the Fundamental Research Funds for the Central Universities under Grant DUT16QY33, by the Scientific Research Starting Foundation for the Returned Overseas Chinese Scholars, and by the Xinghai Scholars Program. The review of this paper was coordinated by Dr. K. Yu.

The authors are with the Faculty of Electronic Information and Electrical Engineering, Dalian University of Technology, Dalian 116023, China (e-mail: wangjie@dlut.edu.cn; zxiao@mail.dlut.edu.cn; qhgao@dlut.edu.cn; xrui.ma@mail.dlut.edu.cn; fengxy@mail.dlut.edu.cn; whyu@dlut.edu.cn).

Color versions of one or more of the figures in this paper are available online at http://ieeexplore.ieee.org.

Digital Object Identifier 10.1109/TVT.2016.2555986

evaluate the proposed schemes on 802.15.4 Zigbee hardware testbeds in two indoor scenarios. Experimental results show that compared with the traditional time-domain feature, the location estimation and activity recognition accuracy using the wavelet feature is remarkably enhanced.

The main contributions of this paper can be summarized as follows.

1) We propose realizing DFLAR using a wavelet feature. The wavelet feature characterizes the shadowing effect in both the time domain and the frequency domain. It could provide in-depth robust discriminative shadowing effect information incurred by a target that is located at different locations or performs different activities. Thus, the wavelet-based DFLAR could achieve significantly better performance.
2) We propose a two-stage strategy to realize multitarget DFLAR. First, we realize target detection and coarse location estimation using a geometry method. Then, with this information as a constraint, we realize accurate localization and activity recognition simultaneously with the softmax regression algorithm for each target one by one. The two-stage strategy makes it feasible to realize multitarget DFLAR with a traditional single-target feature map.
3) We perform experiments with two hardware testbeds and evaluate the proposed schemes extensively under different scenarios and different conditions.

The rest of this paper is structured as follows. Section II reviews the related work on DFL and DFAR. Section III presents the problem formulation and motivation behind the proposed schemes. Section IV introduces the detailed methodology of the proposed DFLAR system. Section V validates the proposed schemes with experimental evaluations. Finally, the conclusion is summarized in Section VI.

II. Related Work

Due to its attractive potential application in several context-aware scenarios, e.g., smart city, smart space, smart house, security safeguard, and ambient intelligence, DFL and DFAR have drawn considerable attention in recent years. Believe that in the near future, these techniques will turn the traditional wireless networks into context-aware intelligent networks with the ability of perceiving the location or activity of the target within its deployment area.

The idea of DFL was independently proposed by Zhang *et al.* [1]–[5] and Youssef *et al.* [6]–[9]. Zhang *et al.* [1]–[3] presented a rectangle model to characterize the feature of wireless links and used a geometric method to realize location estimation. More recently, they also explored a multitarget DFL technique [4] utilizing support vector machine and a measurement-free DFL technique [5] that could estimate the location of reference nodes automatically. Their pioneering work lays the foundation for a model-based DFL technique. Inspired by their work, an elliptical model [10]–[18] and an exponential model [19], [20] have also been adopted to relate the RSS measurement information with target locations. Youssef *et al.* [6]–[9] formulated DFL as a fingerprint-matching question. They built an offline radio map to store the feature of wireless link signal by placing the target at every possible location within the deployment area and estimate the target's location with machine learning methods. Their groundbreaking work provides the basis for a training-based DFL technique. Following their work, Zhao *et al.* [21] utilized histograms to record the RSS feature of every link. Xiao *et al.* [22] generalized the radio map to channel-state-information-based DFL. Zheng *et al.* [23] made valuable exploration on utilizing channel state information to realize localization and achieve accurate localization performance. Hong and Ohtsuki [24] explored the signal-eigenvector-based DFL. The aforementioned work makes valuable exploration on the DFL technique and achieves important research progress. However, the aforementioned work uses only the time-domain feature, i.e., the mean, variance, or peak-to-peak value of the time-domain RSS information, as observation information. As we know, time-domain information is sensitive to environmental noise. To solve this problem and realize robust DFL, we explore utilizing a robust wavelet feature in both the time domain and the frequency domain to improve the system performance.

Recent advances in the DFL technique have enabled wireless networks to passively sense not only the location of a target but the activity of the target, which is named DFAR [25], as well. Essentially, from the methodology point of view, DFAR is similar to the training-based DFL technique. It builds an offline radio feature map to store the feature of wireless link signal with a target that locates at every possible location and performs each feasible activity and estimates the target's location and activity online with machine learning methods. Its difference with the training-based DFL technique is that the categories that need to be classified significantly increase, which makes it a far more challenging problem than DFL. Sigg *et al.* [26]–[28] performed in-depth research on the DFAR problem and proved that DFAR can be realized even with ambient wireless signal. Shi *et al.* [29], [30] explored the methodology of realizing DFAR with FM signal. Wang *et al.* [31] examined the features of channel state information and developed a novel method to identify both in-place activities and walking movements using fine-grained signatures. Wei *et al.* [32] also used channel state information to recognize different activities and investigated the impact of radio frequency interference on its performance. As we know, the complexity of the radio feature map building process exponentially increases with the number of targets. Thus, it is challenging to realize multitarget DFAR. In this paper, we present a two-stage strategy to solve the aforementioned problem and realize DFLAR with a traditional single-target feature map. The first stage differentiates different targets. Then, the second stage realizes the localization and activity recognition of each target one by one. This strategy makes the complexity of the system linear with the number of targets.

III. Problem Formulation and Motivation

A. Problem Formulation

As shown in Fig. 1, two targets within the deployment area of the networks will shadow some of wireless links, i.e., links from nodes 1 to 5, 1 to 6, 2 to 8, and 4 to 6, thus resulting in the variation of the RSS of these links. When targets are

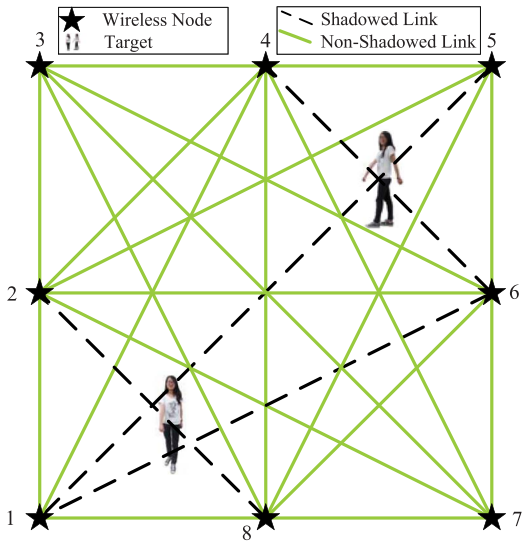

Fig. 1. DFLAR system consisting of eight nodes.

located at different locations or perform different activities, the shadowing effect will be different. Thus, it is feasible to estimate the target's location and activity with RSS measurements. Consider a wireless network consisting of D wireless nodes. Suppose all nodes can communicate with each other, altogether, there are $J = D(D-1)/2$ wireless links. Given RSS measurements of the networks $\mathbf{R}_{0,\ldots,t} = \{\mathbf{R}_0, \ldots, \mathbf{R}_t\}$, where $\mathbf{R}_0 = \{\mathbf{R}_0^j | j = 1, \ldots, J\}$ represent the reference RSS measurements acquired when the deployment area is vacant, and $\mathbf{R}_t = \{\mathbf{R}_t^j | j = 1, \ldots, J\}$ represent the RSS measurements acquired at time t. The objective of the DFLAR system is to estimate the target's location $\mathbf{x}_t^k = (X_t^k, Y_t^k)$ and its activity $\mathbf{a}_t^k$ with location information of the wireless nodes, the total number of targets within the deployment area N, and variation of RSS measurements $\Delta\mathbf{R}_t$, where $\Delta\mathbf{R}_t = \{\mathbf{R}_t^j - \mathbf{R}_0^j | j = 1, \ldots, J\}$.

B. Motivation

Here, we present some intuition on why DFLAR is feasible and why wavelet feature is a discriminative feature for DFLAR. We put two nodes on top of tripods with a height of 1.2 m and a distance of 6 m. The nodes are turned to work on 2.45 GHz. One node transmits a packet to another with a speed of 100 packets per second. We record the RSS with a person standing at the middle point of the link and performing different activities, i.e., squat and rise, stand still, swing of the arm, and walk around. We utilize three most commonly used features, i.e., mean, variance, and peak-to-peak value of the variation of the RSS signal, as the time-domain feature. We also perform wavelet transformation on the variation of RSS measurements and transform the time-domain signal into the time and frequency domains. The principle and advantage of wavelet transformation are shown in Fig. 2(a) and (b). Compared with traditional frequency-domain transformation, e.g., Fourier transformation, wavelet transformation could provide both time and frequency information at the same time. It could analyze a signal at different frequencies with different resolutions. Therefore, fine time resolution and poor frequency resolution at high frequencies and fine frequency resolution and poor time resolution at low frequencies is provided. Hence, compared with the acquired time-domain signal and the frequency-domain signal generated by Fourier transformation, the time- and frequency-domain signal generated by wavelet transformation is more informative and could provide discriminative information for the DFLAR system. In the wavelet domain, we adopt the number of ZCPs, variance, and energy of the coefficient vector corresponding to the cA4 frequency band and the cD4 frequency band to build the feature vector. The number of ZCPs can characterize whether an activity performs fast or slowly in a frequency band, e.g., "walk around" activities occurs more quickly than other activities. The results in Fig. 2(d) confirm this. The variance can characterize the exercise amplitude of an activity, e.g., "squat and rise" activity should demonstrate larger variance than other activities. The results in Fig. 2(d) also confirm this observation. As for the energy, it measures the energy in a frequency band. Fig. 2(d) shows that the "squat and rise" activity has large energy in the cD4 frequency band and small energy in the cA4 frequency band; this is because the "squat and rise" activity performs at a frequency that is close to the frequency of the cD4 band. When performing the "stand still" activity, the target remains motionless. Therefore, it should have small energy in both cA4 and cD4 frequency bands. The results in Fig. 2(d) confirm this as well. In Fig. 2(c) and (d), we can discover that compared with time-domain features, the difference of wavelet features between different activities becomes remarkable. Thus, the recognition task becomes easier. Through these preliminary results, we can see that the proposed wavelet feature is discriminative and robust. Therefore, with the wavelet feature, the performance of the DFLAR system is sure to improve.

IV. Methodology

A. System Overview of DFLAR

The system overview of the proposed wavelet-feature-based two-stage DFLAR system is shown in Fig. 3. The system primarily consists of the following function modules: feature extraction module, which calculates the wavelet feature according to the acquired RSS measurements; target detection and DFL module, which estimates the coarse locations of the targets based on the RSS measurements; and softmax-regression-based DFLAR module, which utilizes the principal component analysis (PCA) algorithm [33] to reduce the dimension of the feature and uses the softmax regression algorithm [34] to classify different locations and activities for each target with coarse location information as a constraint. We will present a detailed implementation of each module in the following sections. It should be mentioned that the proposed DFLAR system is, in fact, a machine learning system. Thus, it needs a training process to build the feature map offline. Then, it realizes online location and activity recognition with the feature map.

B. Feature Extraction

At each time t, after acquiring the RSS measurement of $\mathbf{R}_t^j$ for each link j, we get the variation of the RSS $\Delta\mathbf{R}_t^j$ by

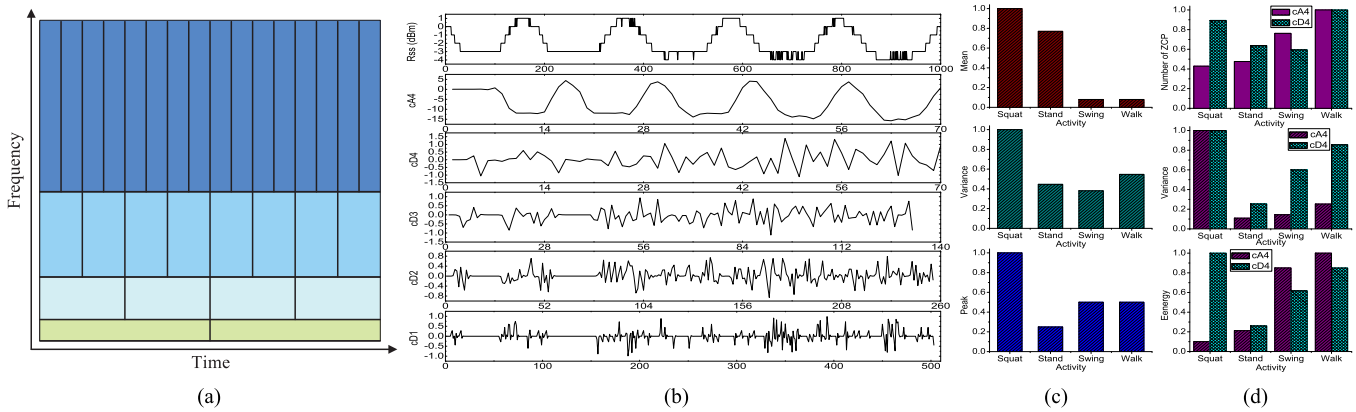

Fig. 2. Wavelet feature. (a) Principle of wavelet decomposition. (b) Wavelet decomposition of the variation of RSS measurements with a "squat and rise" activity. (c) Time-domain features for different activities. (d) Wavelet features for different activities.

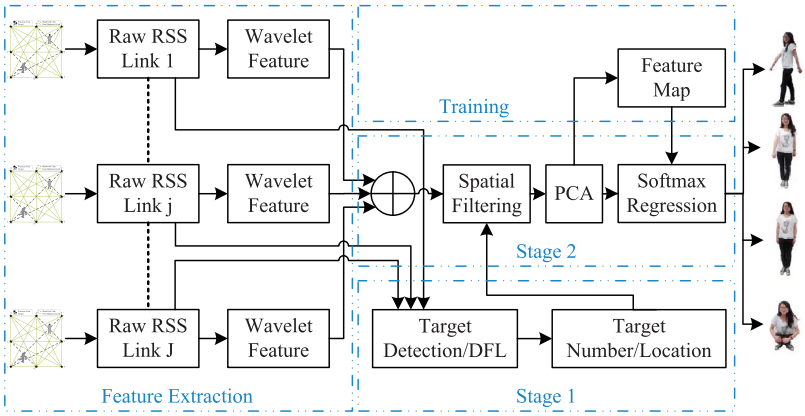

Fig. 3. System overview of the wavelet-feature-based two-stage DFLAR system.

subtracting the reference RSS measurement $\mathbf{R}_0^j$ as follows:

$$\Delta\mathbf{R}_t = \left\{\Delta\mathbf{R}_t^j = \mathbf{R}_t^j - \mathbf{R}_0^j | j = 1, \ldots, J\right\}. \tag{1}$$

The variation of RSS measurements $\Delta\mathbf{R}_t$ is defined as the raw RSS and will be utilized to calculate the wavelet feature and to realize target number detection and DFL.

Wavelet is an effective mathematical tool for time–frequency analysis. It could transform time-domain signals into different frequency subbands as follows:

$$\Psi(\tau, \eta) = \frac{1}{\sqrt{|\eta|}} \int \Delta\mathbf{R}_t \psi\left(\frac{t-\tau}{\eta}\right) dt \tag{2}$$

where $\psi(t)$ represents the mother wavelet that is a prototype for generating other window functions and $\int \psi(t)dt = 0$, η indicates the scale parameter that determines the frequency region, and τ determines the shifted time of the signal. With different values of η and τ, we can reveal the signal structure in different time and frequency windows and generate an over-complete representation of the raw signal. This property makes it particularly suitable for being utilized to extract features from signals to realize the classification task.

In this paper, we use Daubechies wavelets, which are a family of orthogonal wavelets defining a discrete wavelet transform (DWT) [35]. A Daubechies wavelet is often referred to as Dn, where n represents the size of the mother wavelet. It is extensively adopted in DWT since its wavelet coefficients could capture most of the signal energy. Given the variation of RSS measurements $\Delta\mathbf{R}_t$ of length W, DWT proceeds in $\log_2 W$ steps at most and divides the time-domain signal into $\log_2 W$ subbands. It begins with $\Delta\mathbf{R}_t$ and produces two sets of wavelet coefficient vector, i.e., the detailed coefficient vector $cD1$ and the approximation coefficient vector $cA1$, by convolving $\Delta\mathbf{R}_t$ with a high-pass filter $\mathbf{H}$ and a low-pass filter $\mathbf{G}$, followed by a downsampling operation that keeps the length of $cD1$ and $cA1$ be $W/2$. The next step decomposes $cA1$ into two parts $cD2$ and $cA2$ using the same method. The aforementioned procedure repeats until completing the expected level of decomposition. Specifically, in this paper, we use the $D10$ wavelet with the coefficients of the high-pass filter $\mathbf{H}$ and the low-pass filter $\mathbf{G}$ defined by $\mathbf{H} = (0.003, -0.012, -0.006, 0.077, -0.032, -0.242, 0.138, 0.724, 0.604, 0.160)$ and $\mathbf{G} = (-0.160, 0.604, -0.724, 0.138, 0.242, -0.032, -0.078, -0.006, 0.013, 0.003)$. Fig. 2(a) shows the variation of RSS measurements $\Delta\mathbf{R}_t$ of length 1000 and the corresponding wavelet coefficients $cA4$, $cD4$, $cD3$, $cD2$, and $cD1$. In the figure, we can see that the signal feature is primarily implied in $cA4$ and $cD4$. Thus, we build features based on the time-domain wavelet coefficients in these two frequency subbands. Specifically, we adopt the number of ZCPs, variance, and energy of $cA4$ and $cD4$ to build the feature for the DFLAR system.

Suppose a coefficient sequence with length L is $[c_1, c_2, \ldots, c_l, \ldots, c_L]$, point l is detected as a ZCP if the following condition is met:

$$(c_l - \overline{c}) \times (c_{l+1} - \overline{c}) < 0 \tag{3}$$

where $\overline{c}$ represents the mean value that is calculated as follows:

$$\overline{c} = \frac{\sum_{l=1}^{L} c_l}{L}. \tag{4}$$

The variance σ_c of the coefficient sequence is defined by

$$\sigma_c = \frac{\sum_{l=1}^{L} (c_l - \overline{c})^2}{L}. \tag{5}$$

The energy e_c of the coefficient sequence is determined by

$$e_c = \sum_{l=1}^{L} c_l^2. \tag{6}$$

With the number of ZCPs, variance, and energy of $cA4$ and $cD4$, we get a 6×1 feature vector to characterize a wireless link. For the networks composed of J links, we utilize a $6J \times 1$ feature vector F to characterize the feature of the networks. Since F is made up of different statistical metrics that have different physical units, it should be normalized to form a robust feature vector.

C. Stage 1: Target Detection and DFL

The goal of stage 1 is to estimate coarse locations of the targets rapidly with a few simple operations, thus making it feasible to estimate the location and activity of each target accurately in stage 2.

When a target stands near a wireless link, it will shadow the link and cause the RSS drop to some extent. Thus, it is feasible to detect whether a link is shadowed or not as follows:

$$s_t^j = \begin{cases} 1, & \text{if } \left(\Delta \mathbf{R}_t^j < \widetilde{R}\right) \\ 0, & \text{else} \end{cases} \tag{7}$$

where $\widetilde{R}$ represents a threshold value, and the shadowing state $s_t^j = 1$ indicates that link j is shadowed. For a target k, we define an equivalent distance metric d_{kj} to evaluate the distance between target k and link j as follows:

$$d_{kj} = d_{kj1} + d_{kj2} - d_j \tag{8}$$

where d_{kj1}, d_{kj2}, and d_j represent the Euclidean distance between target k and node 1 of link j, target k and node 2 of link j, and nodes 1 and 2 of link j, respectively.

We adopt the elliptical model with a width of λ to represent the effective region of a link. For link j and position k, if the equivalent distance $d_{kj} < \lambda$, it indicates that position k is within the effective region of link j. If a target locates at position k, a link j must be shadowed if $d_{kj} < \lambda$, and *vice versa*. Thus, it is feasible to estimate target location based on the shadowed links. A target will be more likely to locate at position k if position k is within the effective region of multiple shadowed links. Based on the detected shadowed links, we can estimate the probability that a target locates at every predefined location. Thereafter, build the target distribution map $\{P_k | k = 1, \ldots, K\}$ with a lightweight scheme, as shown in Algorithm 1.

Algorithm 1: Target detection and coarse DFL

Input:
Detected shadowed link j, where $j = 1, \ldots, J'$;
Locations of the wireless nodes;
Total number of target N;
Locations of the training point k, where $k = 1, \ldots, K$;
Output:
Feasible locations and their corresponding feasible link set;

```
Initialization:
for k = 1 to K do
    P_k = 0;
end
Build target distribution map:
for j = 1 to J' do
    for k = 1 to K do
        Calculate d_kj with Eq. (8);
        if d_kj < λ then
            P_k = P_k + 1;
        end
    end
end
Detect feasible locations:
for n = 1 to N do
    k̂ = arg max P_k, where k = 1, ..., K;
    P_k̂ = 0;
    if k̂ is not the neighbor node of other feasible locations then
        Record the feasible location and its corresponding feasible link set;
    else
        n = n − 1;
    end
end
```

Target distribution map $\{P_k | k = 1, \ldots, K\}$ characterizes the probability distribution of the targets. If the probability at position k is remarkably larger than others, it indicates that a target may locate at position k with a high possibility. We select N positions that are not next to each other and have N largest probabilities as the coarse locations of the targets. Since we know the coarse location of the target, there is no need to utilize the feature vectors built by all the links for DFLAR. We use only the feature vectors built by the feasible link set, which is defined as follows.

Definition 1: The feasible link set S_k of position k is defined as a maximal set of links in which every link satisfies the condition that position k is within its effective region.

The benefit of utilizing a feasible link set to build a feature vector is twofold. On one hand, we can eliminate the mutual interference between multitarget to some extent since the proposed scheme essentially performs spatial filtering on the links and selects the most related features implied in the feasible links. On the other hand, we can build the feature map offline with only one target that locates at every possible location and performs predefined activities, which remarkably reduces the complexity of a multitarget DFLAR system. Although the proposed system could realize multitarget DFLAR, different from the existing work, it no longer needs to train the system with multiple targets located at multiple positions and perform different activities. Thus, it makes the multitarget DFLAR system more practical.

D. Stage 2: Softmax-Regression-Based DFLAR

Since we know the coarse location information of the targets, we will realize the DFLAR of each target one by one. Thus, the multitarget DFLAR problem is simplified to a single-target

DFLAR problem. We will present the detailed implementation of DFLAR for one target in the following sections.

As previously mentioned, we utilize the number of ZCPs, variance, and energy of $cA4$ and $cD4$ to form a 6×1 feature vector to characterize the wavelet feature of a wireless link. For the networks composed of J links, the wavelet feature vector for the networks is a $6J \times 1$ vector F. With a feasible location $\mathbf{x}_t^k = (X_t^k, Y_t^k)$ and its feasible link set S_k, we perform spatial filtering on the raw wavelet feature vector F. The spatial filtering task can be carried out with a series of simple comparison operations. In brief, if a link is within the feasible link set S_k, we keep the six wavelet features corresponding to this link unchanged. Otherwise, we replace the six wavelet features with values of 0. After performing the spatial filtering task, we get the filtered wavelet vector $\overline{F}$. We will utilize $\overline{F}$ to build the feature map and realize DFLAR. It should be mentioned that when building the feature map in the offline training phase, since we know the actual position of the target, the feasible link set is built based on the known location information. However, when performing the DFLAR task, we use the target detection and the DFL technique presented in Section IV-C to estimate the coarse location and build a feasible link set with the coarse location information.

Now, the DFLAR problem becomes how to estimate target location and its activity with the filtered wavelet vector $\overline{F}$ and the wavelet feature map defined as follows:

$$\mathbf{F} = \left\{ \overline{F}_k^{a,m} | k = 1, \ldots, K; a = 1, \ldots, A; m = 1, \ldots, M \right\} \tag{9}$$

where K represents the total number of training positions, A indicates the total number of activities, and M is the number of training sets for each position or activity. $\overline{F}_k^{a,m}$ is a $6J \times 1$ vector, and $\mathbf{F}$ is a $6J \times KAM$ matrix. Essentially, the goal of the DFLAR problem can be formulated as a minimization problem as follows:

$$\begin{aligned} (\hat{k}, \hat{a}) = \arg \min_{k,a,m} & \left\| \overline{F} - \overline{F}_k^{a,m} \right\| \\ s.t. \quad & k = 1, \ldots, K \\ & a = 1, \ldots, A \\ & m = 1, \ldots, M \end{aligned} \tag{10}$$

where $\hat{k}$ indicates the index of the training position that determines the target location, and $\hat{a}$ represents its activity.

In this paper, we use the machine learning method to solve the aforementioned task. Specifically, we adopt the softmax regression algorithm to perform classification. Meanwhile, to reduce the computational complexity, we use the PCA algorithm to extract the most discriminative features and reduce the dimension of the feature vectors.

PCA [33] is an effective tool to rotate the axes of high-dimensional space to low-dimensional space while keeping the discriminative ability of the data set by ensuring the high variances on the principal axes. With feature map $\mathbf{F}$, we first standardize each row variable. Then, we calculate the covariance matrix $\mathbf{F}\mathbf{F}^T$, where $'T'$ indicates the transposition operation. After performing eigenvalue decomposition on the covariance matrix, we select the Q eigenvectors corresponding to the Q largest eigenvalues to form the $Q \times 6J$ mapping matrix of PCA. The value of Q is determined by the contribution rate α, which represents the ratio of the sum of the Q largest eigenvalues to the sum of the total $6J$ eigenvalues. With the mapping matrix, we can project a high-dimensional $6J \times 1$ feature vector to a $Q \times 1$ vector, thus reducing the dimension of the classification problem.

Softmax regression [34] is a supervised learning algorithm that can realize multiclass classification. Compared with other multiclass classification algorithms, it could output the probabilities that the input vector belongs to each class. Meanwhile, it is more suitable for classifying mutually exclusive classes, e.g., the DFLAR problem. For the DFLAR problem, the input vector is a $Q \times 1$ feature vector, there are KA classes, and, altogether, we have KAM training samples. Softmax regression is the generalization of the well-known logistic regression. Given an input feature vector, it could estimate the probability that $p(y_k^{a,m} = c|\overline{F}_k^{a,m})$ for each value of $c = 1, \ldots, KA$, i.e., it could estimate the probability of the output class label y taking on each of the KA class. The hypothesis of the softmax regression model is defined by (11), shown at the bottom of the page, where θ_c is a $Q \times 1$ vector that represents the model parameter for the cth output, and $\theta = [\theta_1, \theta_2, \ldots, \theta_{KA}]^T$ is a $KA \times Q$ parameter matrix for the softmax regression model.

The cost function of the softmax regression algorithm is defined by (12), shown at the bottom of the page, where $1\{\cdot\}$ is an indicator function with $1\{\text{true}\} = 1$ and $1\{\text{false}\} = 0$, KAM represents the total number of training samples, KA is the number of classes, β determines the proportion of the weight decay term, and θ_{cq} represents the qth element of vector θ_c. The cost function $\Phi(\theta)$ is strictly convex, and we can solve the model parameter θ with the gradient descent algorithm with the derivative determined by (13), shown at the bottom of the next page. With the softmax regression model, for any measured wavelet feature vector $\overline{F}$, it is straightforward to calculate $\theta \times \overline{F}$, thus

$$h_\theta\left(\overline{F}_k^{a,m}\right) = \begin{bmatrix} p\left(y_k^{a,m} = 1 | \overline{F}_k^{a,m}; \theta\right) \\ p\left(y_k^{a,m} = 2 | \overline{F}_k^{a,m}; \theta\right) \\ \vdots \\ p\left(y_k^{a,m} = KA | \overline{F}_k^{a,m}; \theta\right) \end{bmatrix} = \frac{1}{\sum_{c=1}^{KA} e^{\theta_c^T \overline{F}_k^{a,m}}} \begin{bmatrix} e^{\theta_1^T \overline{F}_k^{a,m}} \\ e^{\theta_2^T \overline{F}_k^{a,m}} \\ \vdots \\ e^{\theta_{KA}^T \overline{F}_k^{a,m}} \end{bmatrix} \tag{11}$$

$$\Phi(\theta) = -\frac{1}{KAM} \left[\sum_{m=1}^{M} \sum_{a=1}^{A} \sum_{k=1}^{K} \sum_{c=1}^{KA} 1\left\{ y_k^{a,m} = c \right\} \log \frac{e^{\theta_c^T \overline{F}_k^{a,m}}}{\sum_{l=1}^{KA} e^{\theta_l^T \overline{F}_k^{a,m}}} \right] + \frac{\beta}{2} \sum_{c=1}^{KA} \sum_{q=1}^{Q} \theta_{cq}^2 \tag{12}$$

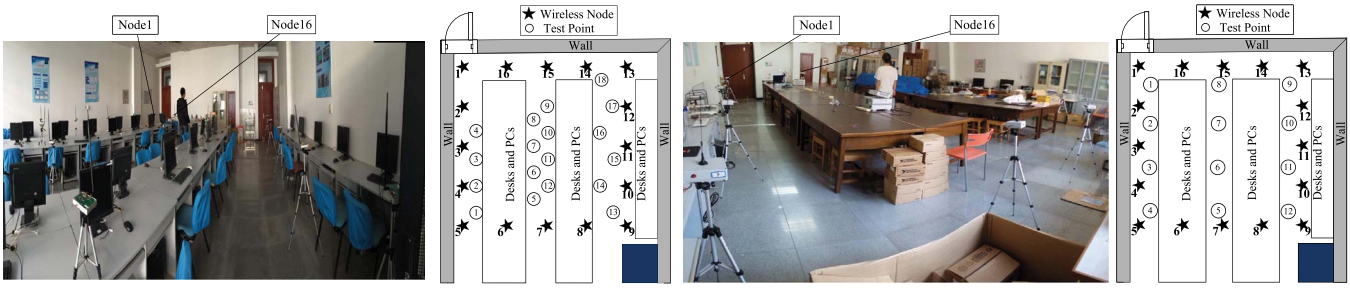

Fig. 4. Layout and photographs of the two experiments. (a) Scenario of the first experiment. (b) Network geometry of the first experiment. (c) Scenario of the second experiment. (d) Network geometry of the second experiment.

achieving the probability of being recognized to each class. Suppose the cth class has maximum probability, then $\mathbf{x}_t^c = (X_t^c, Y_t^c)$, and $\mathbf{a}_t^c$ corresponding to the cth class is recognized as the location and activity of the target. It should be mentioned that the location estimation information may be wrong in the first stage. To improve the robustness of the system, we use the softmax regression model to calculate the probabilities of each class by supposing that the target locates at the estimated position in the first stage or at its neighboring positions. Moreover, the class with maximum probability is adopted as the final estimation.

V. Experimental Evaluation

A. Description of the Experiment

We design two prototype networks to evaluate the performance of the proposed schemes. One network is comprised of 17 nodes that are equipped with CC2520 and MSP430F5438 chipsets. Another network is comprised of 17 nodes that are equipped with a CC2530 chipset. Nodes 1–16 are normal nodes that perform a link-scanning task. Node 17 acts as the central node that acquires all the RSS measurements. The nodes work on the frequency of 2.45 GHz and with a transmission power of 5 dBm. We use a token-passing protocol to coordinate the link-scanning process and the operating mode of the normal nodes. Each normal node transmits the RSS measurements acquired in the last scanning cycle in turn according to their ID number. All the other normal nodes receive the signal and measure the RSS of the transmitting node. The central node monitors all the network traffic and feeds the RSS data to the PC via a universal asynchronous receiver/transmitter port. We deploy the two prototype networks in two laboratory rooms. The layout and photographs of the two deployment areas are shown in Fig. 4. The normal nodes are placed 1.8 m apart along the perimeter of a 7.2 m $\times$ 7.2 m square area. Two experiments are performed in these two challenging cluttered indoor scenarios with several desks and PCs within the deployment area.

By default, we use only eight normal nodes (choose one every other node as shown in Fig. 4) to realize the DFLAR of one target. The default parameters of the algorithms are summarized as follows: The contribution rate of PCA $\alpha = 0.98$, the proportion of the weight decay term for the cost function $\beta = 0.01$, width of the elliptical model $\lambda = 0.09$ m, and the threshold value for shadowing state detection $\widetilde{R} = -2$ dBm. If both the estimated location and activity are right, we say that the DFLAR system identifies the status correctly. We use the percentage of the number of correctly estimated status to the total number of tested status as the accuracy metric to evaluate the schemes. In the first experiment, there are 18 feasible locations, and the target may perform one of four possible activities, i.e., squat and rise, stand still, swing of the arm, and walk around, in every location. In the second experiment, there are 12 feasible locations, and the target may perform one of four possible activities in every location as in the first experiment. In the experiments, the time duration during which we record data when a target locates at a position and performs one activity is 4 s. The link measurements acquired within 4 s form a

TABLE I
Comparison of Accuracy

Accuracy(%)		T-DFLAR	TF-DFLAR	W-DFLAR
1st experiment	DFLAR	78.3	84.2	90.0
	DFL	92.4	94.7	95.2
2nd experiment	DFLAR	79.1	88.3	95.4
	DFL	96.3	97.6	99.5

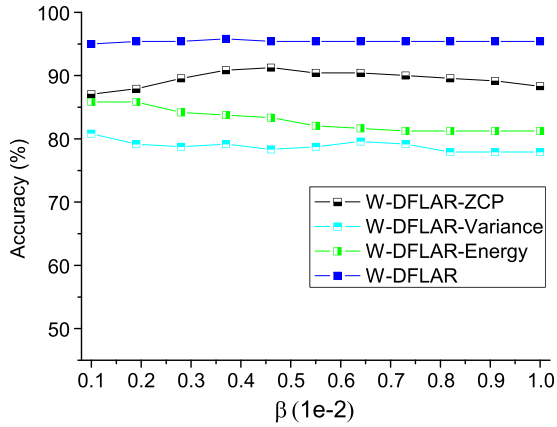

Fig. 5. Performance with each wavelet feature in the second experiment.

$$\nabla_{\theta_c}\Phi(\theta) = -\frac{1}{KAM}\sum_{m=1}^{M}\sum_{a=1}^{A}\sum_{k=1}^{K}\left[\overline{F}_k^{a,m}\left(1\left\{y_k^{a,m}=c\right\} - p\left(y_k^{a,m}=c|\overline{F}_k^{a,m};\theta\right)\right)\right] + \beta\theta_c \tag{13}$$

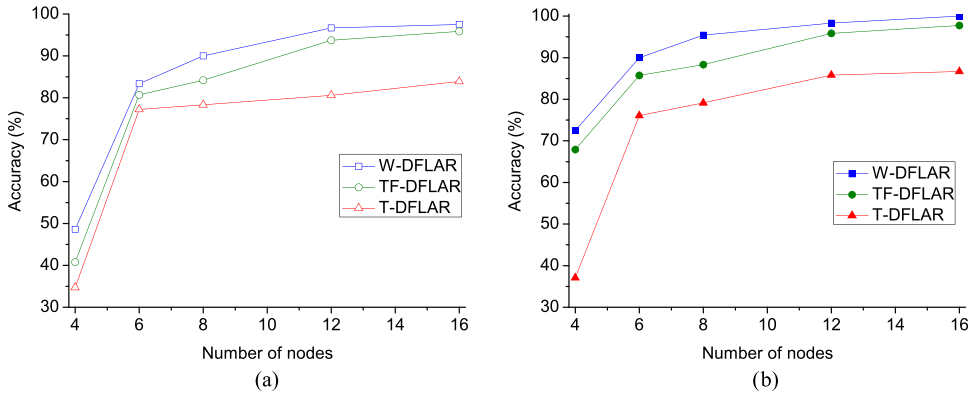

Fig. 6. Performance with different numbers of nodes. (a) First experiment. (b) Second experiment.

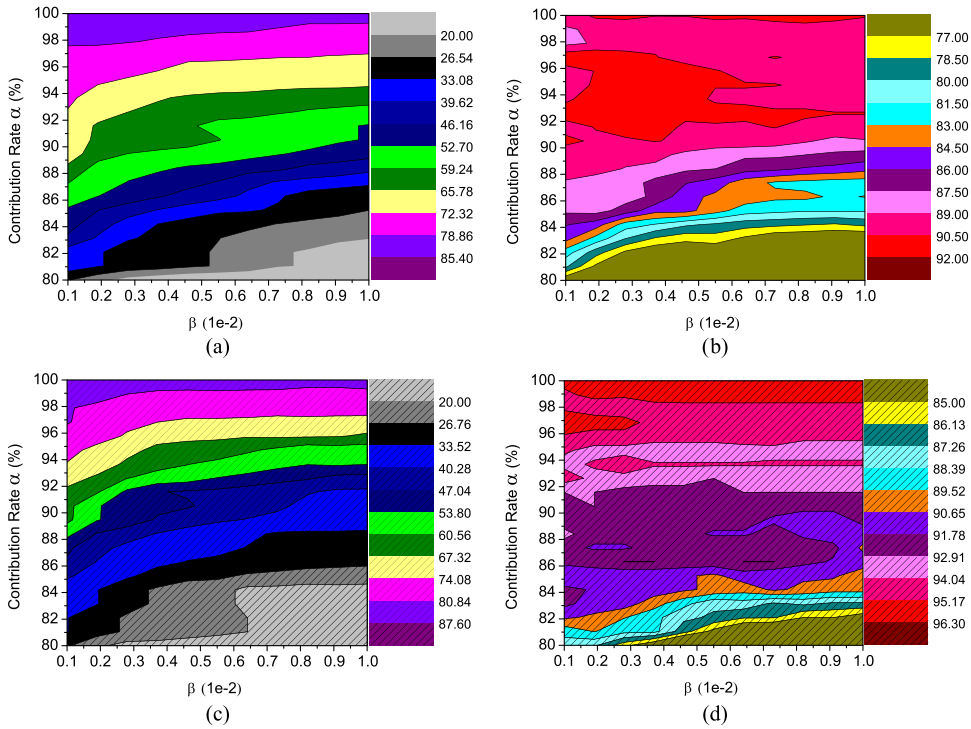

Fig. 7. Performance with different values of the contribution rate of PCA α and the proportion of the weight decay term for the cost function β. (a) Performance of T-DFLAR in the first experiment. (b) Performance of W-DFLAR in the first experiment. (c) Performance of T-DFLAR in the second experiment. (d) Performance of W-DFLAR in the second experiment.

training set or a test set. We use six training sets and five test sets for each status.

B. Performance Overview

To evaluate the performance of the proposed wavelet-based DFLAR system, we compare it with the traditional time-domain-feature-based system and the time- and frequency-domain-based system that also utilizes spectrum energy and entropy of the spectrum as frequency-domain features [28]. We adopt the combination of three most commonly used features, i.e., mean, variance, and peak-to-peak value of RSS signal, as the time-domain feature to realize DFLAR. The wavelet-based DFLAR is abbreviated as W-DFLAR, the time-domain-based DFLAR is abbreviated as T-DFLAR, and the system that utilizes both the three time-domain features and the two frequency-domain features is abbreviated as TF-DFLAR. The accuracy of realizing DFLAR and device-free wireless localization only is summarized in Table I. From the table, we can see that the wavelet feature is a robust and high-performance feature that can improve the location and activity recognition accuracy by almost 15% and 7% when compared with T-DFLAR and TF-DFLAR, respectively. In particular, with the wavelet feature, the performance of DFLAR is close to that of the DFL system, which estimates the target location only.

C. Performance Analysis

We use three features, i.e., number of ZCPs, variance, and energy of the coefficient vector, to build the feature vector for the W-DFLAR system. To explore the contribution of each feature, we evaluate the performance when using only one wavelet feature to realize DFLAR. The result in Fig. 5 reveals that the accuracy is higher than 80% when even utilizing one feature

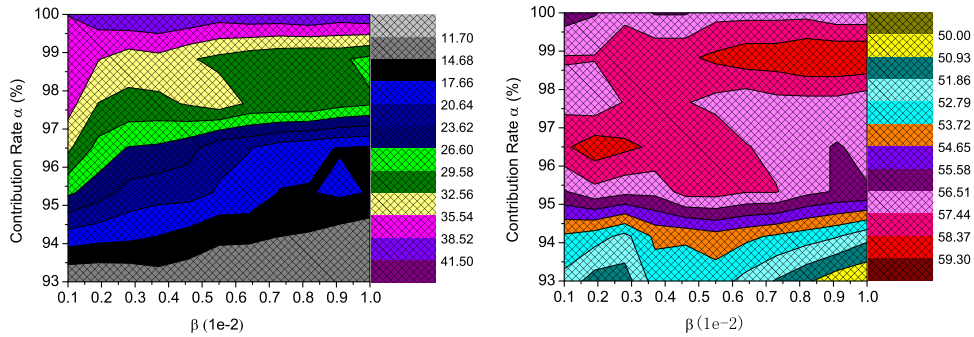

Fig. 8. Multitarget performance with different values of the contribution rate of PCA α and the proportion of the weight decay term for the cost function β. (a) Performance of T-DFLAR in the second experiment. (b) Performance of W-DFLAR in the second experiment.

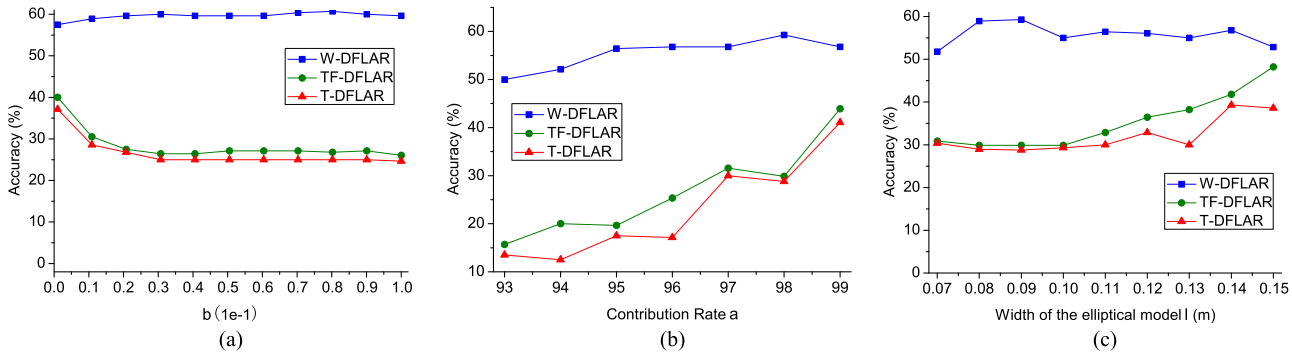

Fig. 9. Multitarget performance with different parameter values. (a) With different contribution rates of PCA α. (b) With different proportions of the weight decay term for the cost function β. (c) With different widths of the elliptical model λ.

only, which confirms the excellent property of the proposed wavelet features.

Since the DFLAR system utilizes the shadowing effect of the target on wireless links to realize location estimation and activity recognition, its performance must be determined by the total number of utilized wireless nodes. We evaluate the performance of the DFLAR system with different numbers of wireless nodes and summarize the result in Fig. 6. It is shown that six nodes are sufficient for the system to achieve acceptable performance for the deployment areas.

The contribution rate of PCA α and the proportion of the weight decay term for the cost function β are two key parameters of the proposed algorithm. We evaluate the proposed DFLAR system by varying these two parameters. Fig. 7 indicates that the performance is sensitive to α. With a larger α value, the performance will be better. Thus, we should select enough eigenvectors to perform PCA to ensure that α is large enough. Fig. 7 also reveals that the algorithm is not very sensitive to β, which makes it convenient to be deployed.

D. Performance Under Multitarget Scenario

We also evaluate the system by letting two targets perform different activities independently and simultaneously at two random locations in the second experimental scenario. The result in Fig. 8 indicates that the W-DFLAR system can achieve an accuracy level of nearly 60% when the contribution rate $\alpha > 98\%$, which is remarkably better than the time-domain-feature-based T-DFLAR. It confirms the excellent property of the wavelet features. We also evaluate the robustness of the system under different parameters. The performance with different values of the contribution rate of PCA α, proportion of the weight decay term for the cost function β, and width of the elliptical model λ is shown in Fig. 9. In the default setting for tracking and recognizing two targets simultaneously, T-DFLAR and TF-DFLAR can achieve an accuracy level of only 28.9% and 30.9%, whereas the proposed wavelet-feature-based W-DFLAR can achieve an accuracy level of 59.3%. If we consider only the location estimation task, T-DFLAR and TF-DFLAR can estimate the target location with an accuracy level of 89.6% and 90.8%, whereas W-DFLAR can achieve an accuracy level of 92.1%.

VI. Conclusion

We have explored the method of realizing DFLAR with the novel wavelet feature. Compared with the existing time-domain feature, the wavelet feature could provide in-depth robust discriminative information in both the time domain and the frequency domain. Thus, with the wavelet feature, the performance of the DFLAR system remarkably improves. Experimental results show that it could achieve simultaneous location and activity recognition accuracy of 95.4% and 59.3% for tracking one and two targets, the corresponding accuracy for the traditional time-domain method being 79.1% and 28.9% and that for the time- and frequency-domain method being 88.3% and 30.9%, respectively. When considering only the location estimation accuracy, the wavelet-feature-based method can achieve an accuracy level of 99.5% and 92.1% for tracking one and two targets, the corresponding accuracy for the

traditional time-domain method being 96.3% and 89.6% and that for the time- and frequency-domain method being 97.6% and 90.8%, respectively. The result confirms that the wavelet feature is a robust and discriminative feature for realizing DFL and activity recognition.

It should be mentioned that realizing multitarget activity recognition simultaneously is still a challenging new task to solve. We only do some exploration in this paper. We will try to improve its accuracy in our future work.

REFERENCES

[1] D. Zhang, J. Ma, Q. Chen, and L. M. Ni, "An RF-based system for tracking transceiver-free objects," in *Proc. IEEE 5th Int. Conf. Pervasive Comput. Commun.*, New York, NY, USA, Mar. 2007, pp. 135–144.

[2] D. Zhang and L. M. Ni, "Dynamic clustering for tracking multiple transceiver-free objects," in *Proc. IEEE 7th Int. Conf. Pervasive Comput. Commun.*, Galveston, TX, USA, Mar. 2009, pp. 1–8.

[3] D. Zhang, Y. Liu, and L. M. Ni, "RASS: A real-time, accurate and scalable system for tracking transceiver-free objects," in *Proc. IEEE 9th Int. Conf. Pervasive Comput. Commun.*, Seattle, WA, USA, Mar. 2011, pp. 197–204.

[4] D. Zhang *et al.*, "Fine-grained localization for multiple transceiver-free objects by using RF-based technologies," *IEEE Trans. Parallel Distrib. Syst.*, vol. 25, no. 6, pp. 1464–1475, Jun. 2014.

[5] D. Zhang, X. Jiang, and L. M. Ni, "Double free: Measurement-free localization for transceiver-free object," in *Proc. IEEE 3rd Int. Conf. Parallel Process.*, Minneapolis, MN, USA, Sep. 2014, pp. 529–538.

[6] M. Youssef, M. Mah, and A. Agrawala, "Challenges: Device-free passive localization for wireless environments," in *Proc. 13th ACM Int. Conf. Mobile Comput. Netw.*, Montreal, QC, Canada, Sep. 2007, pp. 222–229.

[7] M. Moussa and M. Youssef, "Smart devices for smart environments: Device-free passive detection in real environments," in *Proc. IEEE 7th Int. Conf. Pervasive Comput. Commun.*, Galveston, TX, USA, Mar. 2009, pp. 1–6.

[8] A. Saeed, A. Kosba, and M. Youssef, "Ichnaea: A low-overhead robust WLAN device-free passive localization system," *IEEE J. Sel. Topics Signal Process.*, vol. 8, no. 1, pp. 5–15, Feb. 2014.

[9] M. Seifeldin, A. Saeed, A. Kosba, A. El-keyi, and M. Youssef, "Nuzzer: A large-scale device-free passive localization system for wireless environments," *IEEE Trans. Mobile Comput.*, vol. 12, no. 7, pp. 1321–1334, Jul. 2013.

[10] Y. Zhao and N. Patwari, "Noise reduction for variance-based device-free localization and tracking," in *Proc. IEEE 8th Commun. Soc. Conf. Sens., Mesh Ad Hoc Commun. Netw.*, Salt Lake City, UT, USA, Jun. 2011, pp. 179–187.

[11] Y. Zhao and N. Patwari, "Robust estimators for variance-based device-free localization and tracking," *IEEE Trans. Mobile Comput.*, vol. 14, no. 10, pp. 2116–2129, Oct. 2015.

[12] J. Wilson and N. Patwari, "Radio tomographic imaging with wireless networks," *IEEE Trans. Mobile Comput.*, vol. 9, no. 5, pp. 621–632, May 2010.

[13] J. Wang *et al.*, "Transferring compressive sensing based device-free localization across target diversity," *IEEE Trans. Ind. Electron.*, vol. 62, no. 4, pp. 2397–2409, Apr. 2015.

[14] L. Chang, J. Wang, D. Fang, and X. Chen, "NDP: A novel device-free localization method with little efforts," in *Proc. IEEE 13th Int. Conf. Inf. Process. Sens. Netw.*, Berlin, Germany, Apr. 2014, pp. 305–306.

[15] J. Wang *et al.*, "LCS: Compressive sensing based device-free localization for multiple targets in sensor networks," in *Proc. 32th IEEE Int. Conf. Comput. Commun.*, Turin, Italy, Apr. 2013, pp. 145–149.

[16] Z. Yang, K. Huang, X. Guo, and G. Wang, "A real-time device-free localization system using correlated RSS measurements," *EURASIP J. Wireless Comm. Netw.*, vol. 2013, no. 186, pp. 1–12, Jul. 2013.

[17] J. Wang *et al.*, "Robust device-free wireless localization based on differential RSS measurements," *IEEE Trans. Ind. Electron.*, vol. 60, no. 12, pp. 5943–5952, Dec. 2013.

[18] J. Wang, Q. Gao, H. Wang, Y. Yu, and M. Jin, "Time-of-flight-based radio tomography for device free localization," *IEEE Trans. Wireless Commun.*, vol. 12, no. 5, pp. 2355–2365, May 2013.

[19] S. Nannuru, Y. Li, Y. Zeng, M. Coates, and B. Yang, "Radio frequency tomography for passive indoor multi-target tracking," *IEEE Trans. Mobile Comput.*, vol. 12, no. 12, pp. 2322–2333, Dec. 2013.

[20] Y. Guo *et al.*, "An exponential-Rayleigh model for RSS-based device-free localization and tracking," *IEEE Trans. Mobile Comput.*, vol. 14, no. 3, pp. 484–494, Mar. 2015.

[21] Y. Zhao, N. Patwari, J. M. Phillips, and S. Venkatasubramanian, "Radio tomographic imaging and tracking of stationary and moving people via kernel distance," in *Proc. IEEE 12th Int. Conf. Inf. Process. Sens. Netw.*, Philadelphia, PA, USA, Apr. 2013, pp. 229–240.

[22] J. Xiao, K. Wu, Y. Yi, L. Wang, and L. M. Ni, "Pilot: Passive device-free indoor localization using channel state information," in *Proc. 33th Int. Conf. Distrib. Comput. Syst.*, Philadelphia, PA, USA, Jul. 2013, pp. 236–245.

[23] X. Zheng, C. Wang, Y. Chen, and J. Yang, "Accurate rogue access point localization leveraging fine-grained channel information," in *Proc. IEEE Int. Conf. Commun. Netw. Security*, San Francisco, CA, USA, Oct. 2014, pp. 211–219.

[24] J. Hong and T. Ohtsuki, "Signal eigenvector-based device-free passive localization using array sensor," *IEEE Trans. Veh. Technol.*, vol. 64, no. 4, pp. 1354–1363, Apr. 2015.

[25] M. Scholz, S. Sigg, H. R. Schmidkte, and M. Beigl, "Challenges for device-free radio-based activity recognition," in *Proc. 3rd Workshop Context-Syst. Des., Eval. Optim.*, Copenhagen, Denmark, Dec. 2011, pp. 1–12.

[26] S. Sigg, S. Shi, and Y. Ji, "RF-Based device-free recognition of simultaneously conducted activities," in *Proc. 12th ACM Conf. Pervasive Ubiquitous Comput.*, Zurich, Switzerland, Sep. 2013, pp. 531–540.

[27] S. Sigg, U. Blanke, and G. Troster, "The telepathic phone: Frictionless activity recognition from WiFi-RSSI," in *Proc. IEEE 12th Int. Conf. Pervasive Comput. Commun.*, Budapest, Hungary, Mar. 2014, pp. 148–155.

[28] S. Sigg, M. Scholz, S. Shi, Y. Ji, and M. Beigl, "RF-sensing of activities from non-cooperative subjects in device-free recognition systems using ambient and local signals," *IEEE Trans. Mobile Comput.*, vol. 13, no. 4, pp. 907–920, Apr. 2014.

[29] S. Shi, S. Sigg, and Y. Ji, "Joint localization and activity recognition from ambient FM broadcast signals," in *Proc. 12th ACM Conf. Pervasive Ubiquitous Comput.*, Zurich, Switzerland, Sep. 2013, pp. 521–530.

[30] S. Shi, S. Sigg, W. Zhao, and Y. Ji, "Monitoring attention using ambient FM radio signals," *IEEE Pervasive Comput.*, vol. 13, no. 1, pp. 30–36, Jan. 2014.

[31] Y. Wang *et al.*, "E-eyes: Device-free location-oriented activity identification using fine-grained WiFi signatures," in *Proc. 20th Int. Conf. Mobile Comput. Netw.*, Maui, HI, USA, Sep. 2014, pp. 617–628.

[32] B. Wei, W. Hu, M. Yang, and C. T. Chou, "Radio-based device-free activity recognition with radio frequency interference," in *Proc. 14th IEEE Int. Conf. Inf. Process. Sens. Netw.*, Seattle, WA, USA, Apr. 2015, pp. 154–165.

[33] M. Alsheikh, S. Lin, D. Niyato, and H. Tan, "Machine learning in wireless sensor networks: Algorithms, strategies, and applications," *IEEE Commun. Surveys Tuts.*, vol. 16, no. 4, pp. 1996–2018, 4th Quart. 2014.

[34] D. Heckerman and C. Meek, "Models and selection criteria for regression and classification," in *Proc. 13th Int. Conf. Uncertainty Artif. Intell.*, San Francisco, CA, USA, 1997, pp. 223–228.

[35] C. Vonesch, T. Blu, and M. Unser, "Generalized Daubechies wavelet families," *IEEE Trans. Signal Process.*, vol. 55, no. 9, pp. 4415–4429, Sep. 2007.

Jie Wang (M'12) received the B.S. degree from Dalian University of Technology, Dalian, China, in 2003; the M.S. degree from Beijing University of Aeronautics and Astronautics, Beijing, China, in 2006; and the Ph.D. degree from Dalian University of Technology in 2011, all in electronic engineering.

He is currently an Associate Professor with Dalian University of Technology. His research interests include wireless localization and tracking, wireless sensor networks, and cognitive radio networks.

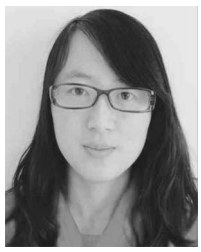

Xiao Zhang received the B.S. degree in electronic engineering from Dalian University of Technology, Dalian, China, in 2014, where she is currently working toward the M.S. degree with the Department of Electrical Engineering.

Her research interests include device-free wireless localization and recognition.

Qinghua Gao received the B.S., M.S., and Ph.D. degrees in electronic engineering from Dalian University of Technology, Dalian, China, in 2003, 2007, and 2012, respectively.

She is currently an Assistant Professor with Dalian University of Technology. Her research interests are in the area of wireless networks, including tracking, localization, and information processing.

Xiaorui Ma received the B.S. degree in applied mathematics from Lanzhou University, Lanzhou, China, in 2008. She is currently working toward the Ph.D. degree with the Department of Electrical Engineering, Dalian University of Technology, Dalian, China.

Her research interests include machine learning and hyperspectral image classification.

Xueyan Feng received the B.S. degree in electronic engineering from Dalian University of Technology, Dalian, China, in 2015, where she is currently working toward the M.S. degree with the Department of Electrical Engineering.

Her research interests include device-free wireless localization and recognition.

Hongyu Wang received the B.S. degree in electronic engineering from Jilin University of Technology, Changchun, China, in 1990; the M.S. degree in electronic engineering from the Graduate School of Chinese Academy of Sciences, Beijing, China, in 1993; and the Ph.D. degree in precision instrument and optoelectronics engineering from Tianjin University, Tianjin, China, in 1997.

He is currently a Professor with Dalian University of Technology. His research interests include algorithmic, optimization, and performance issues in wireless ad hoc, mesh, and sensor networks.